FIRST QUARTERLY REPORT

THE STUDY
OF PLASMA - BOUNDARY INTERACTIONS

(1 September 1967 through 30 November 1967)

GPO PRICE $ _____

CFSTI PRICE(S) $ _____

Hard copy (HC) _____

Microfiche (MF) _____

ff 653 July 65

BY

S. Aisenberg
P. Hu
V. Rohatgi
S. Ziering

APR 1968
RECEIVED
NASA STI FACILITY
INPUT BRANCH

Document Number SSI-455-QR1

SPACE SCIENCES INCORPORATED

FIRST QUARTERLY REPORT

THE STUDY OF PLASMA-BOUNDARY INTERACTIONS

(1 September 1967 through 30 November 1967)

By

S. Aisenberg
P. Hu
V. Rohatgi
S. Ziering

Document Number SSI-455-QR1

ABSTRACT

Experiments have been designed to measure the electrode drag forces in pulsed plasma accelerators and to extend the ~~carbon~~ *previous* electrode drag measurements to higher arc currents (up to a thousand amperes). The Doppler shift technique has been developed to determine the particle speed in the accelerated plasmas. A small wavelength shift of the order of 0.001 Å due to the motion of the radiating particle will be measured with an electrically modulated Fabry-Perot interferometer. To further understand the measured threshold in the electrode drag force, a physical model of threshold in momentum accommodation coefficient, depending on the melting point of surface atoms, has been developed.

CONTENTS

ILLUSTRATIONS

TABLES

1. INTRODUCTION

This report covers the first quarter of a program to study plasma boundary effects. The period covered is essentially from September 1967 through November 1967.

Previous experiments showed that there is an appreciable drag interaction between a magnetically accelerated plasma and the electrodes. In addition, there appears to be a drag threshold in the sense that the drag increases consiserably for large magnetic fields B and currents I. There is also a drag saturation at larger B and I.

In order to extend and interpret the data, measurements are needed for the particle velocity. Since the plasma phase velocity is not necessarily the same as the particle velocity, it was decided to measure the ion and atom velocity directly (as a function of operating parameters) by means of Doppler shift measurements. This report will outline the planned measurement technique.

The interpretation of the threshold drag can be formulated in terms of a threshold in the momentum accommodation coefficient. Calculations of the accommodation coefficient thereshold mechanism are in progress and indicate that the drag threshold should be related to the sputtering threshold and possibly to the melting temperature.

2. EXPERIMENTAL PROGRAM

This section deals with the design of two experiments: (1) to measure the tangential electrode drag from an accelerated plasma pulse at higher pulsed current levels, and (2) to measure the tangential particle velocity in these plasmas using the Doppler shift technique. The details of the experiments are discussed in the following subsections.

2.1 The Drag Measurement from a Pulsed Plasma

Conceptually, the drag measuring experiment is similar to that used earlier for the measurement of electrode drag forces from a continuous arc plasma[1]. This experiment is being designed so that the drag measurements with dc arcs can be extended from 100 amps (reported in Reference 1) to a few thousand amp arcs, in addition to studying the drag forces from pulsed plasma accelerators. These measurements should be of interest especially since the earlier drag measurement indicated certain saturation effects at higher arc currents.

It is planned that in this experiment the drag forces will be measured on both cathode and anode electrodes for several electrode materials and plasma gases. The apparatus is designed to study the pulsed arcs up to 5000 amps in magnetic fields up to about 2000 gauss.

Figure 1 shows the general layout of the apparatus. The movable electrode structure consists of a copper disc 1 cm thick and 2 cm diameter located in the center of the system. The electrode is attached to a torsion spring through a high temperature insulator. This is necessary to prevent the arc heat and voltage from affecting the sensitivity of the spring balance. Additional heat shields are provided to protect the spring balance from hot plasma gases. The electrical connection between the rotary electrode
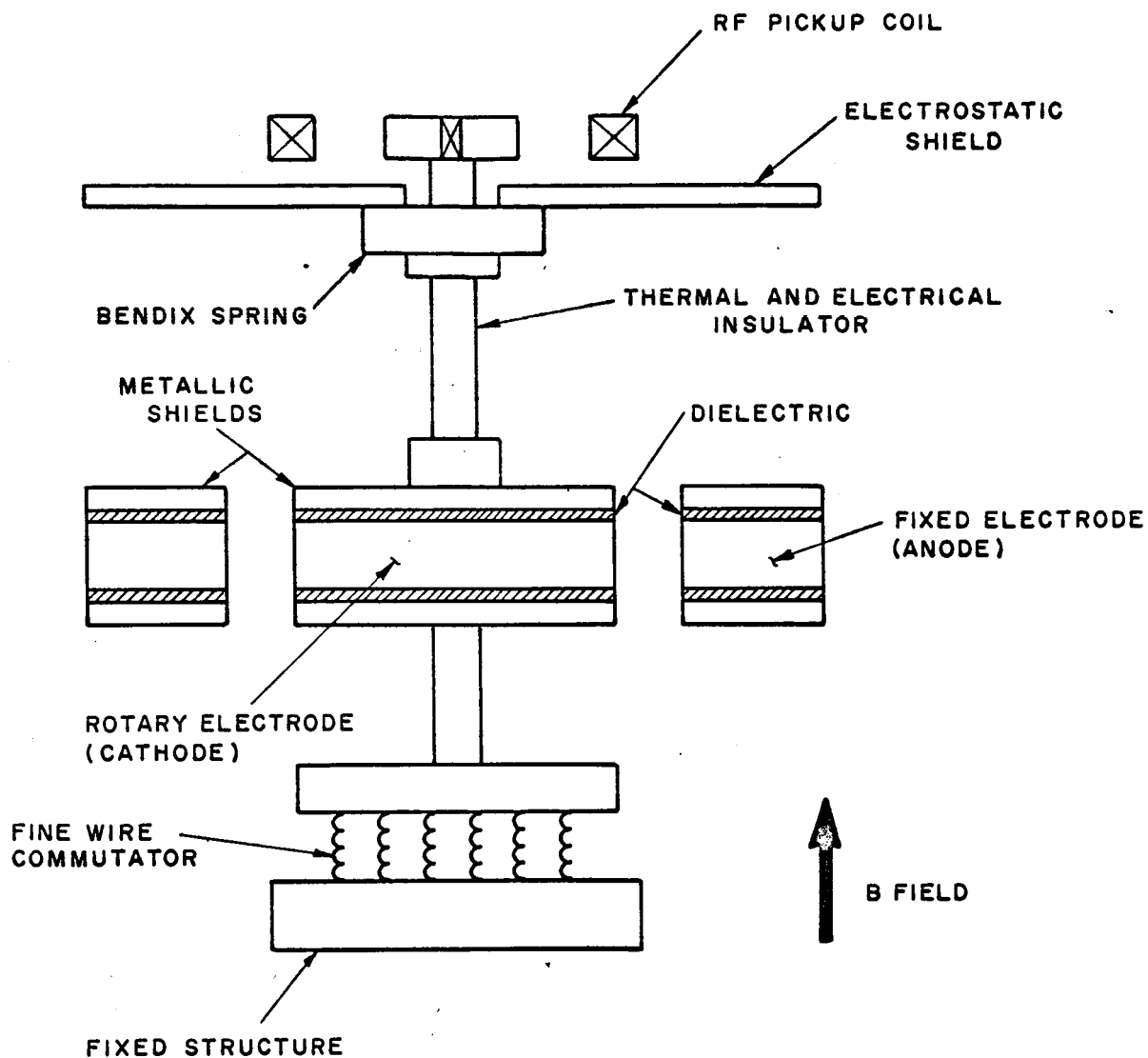
FIGURE 1.

SCHEMATIC DIAGRAM OF THE APPARATUS FOR
MEASURING ELECTRODE DRAG FORCES FROM
PULSED PLASMA ACCELERATION.

structure and the arc power supply is made through a number of fine wires which can carry the arc current and yet not affect the sensitivity of the force transducer. The design of this commutator is discussed in detail in the next section.

The other fixed electrode is made of a water-cooled copper ring about 1 cm thick with an internal diameter of 4 cm. This electrode is placed symmetrically around the rotary electrode so that the arc runs radially through a gap of 1 cm. Provision is made so that either electrode can be operated as cathode, thus making it possible to measure the drag forces on cathode and anode electrodes under similar conditions. The use of magnetic and high vapor pressure materials is avoided in the construction of this apparatus. Most of the hardware consists of non-magnetic stainless steel and copper. To prevent sputtering and sparkover, high temperature dielectric coating and silica tubes are used. The principle of composite metallic and dielectric electrodes[2] is employed to confine the arc in the given plasma volume.

The magnet for the accelerator consists of two stacks of air core, water-cooled coils. A Helmholtz structure is used to generate a uniform field over a large volume. The coils are placed outside the vacuum chamber. The magnet. is energized by a high current dc power supply. A current of 200 amps through the coils produces a field of about 1000 gauss.

The existing vacuum and gas handling system which was made for earlier drag force measurement[3] will also be used in the present experiment. This system consists of a mechanical and a 2-inch air-cooled oil diffusion pump with two zeolite traps located on either side of the diffusion pump. Ultimate vacuum of about 7×10^{-8} Torr has been achieved with this system without the use of liquid nitrogen traps and without bakeout.

2.1.1 High Current Feed to the Rotary Electrode

The liquid metal commutator designed to inject high arc currents into the rotary electrode[1] is not suitable for the pulse drag measurement due to the viscosity of the liquid pool. Similarly a ball bearing commutator is found unsatisfactory due to its high starting torque and contact resistance.

The high arc current to the electrode will therefore be fed by a number of fine wire filaments connected between a fixed and the rotary electrode. These wires have to be very thin so as not to affect the sensitivity of the transducer and yet sufficient in number to carry the high arc current without melting. To find the number and material of wire which will be best suited for this purpose, a figure of merit is defined, by equating the ohmic heating to the heat required to melt the wire. Assuming that the conduction and radiation losses are negligible, we have:

$$\frac{I^2}{A} \rho = s \, d \, A \left(T_m - T_o \right) \tag{1}$$

where,

$\quad I \quad = \quad$ current carried by the conductor,

$\quad \rho \quad = \quad$ resistivity of the conductor,

$\quad A \quad = \quad$ cross-sectional area,

$\quad s \quad = \quad$ specific heat,

$\quad d \quad = \quad$ density,

$\quad T_m \quad = \quad$ melting point, and

$\quad T_o \quad = \quad$ room temperature (= 300°K).

The current density $J = I/A$ which will raise the conductor temperature to the melting point is given by:

$$J = I/A = \left\{ \frac{s \cdot d \cdot (T_m - T_o)}{\rho} \right\}^{1/2}. \qquad (2)$$

The melting point, specific heat, density and the estimated current density J for various materials are listed in Table 1. Also in the same table is listed the modulus of elasticity E, which is necessary to be considered in the selection of material for this purpose.

For the present application, the best material should have high J and low E. Table 1, however, indicates that none of the materials listed satisfy both the requirements simultaneously. Copper has the highest J value but not the lowest value of E. Iridium, on the other hand, has the lowest value of E and also has a low value of J. In general, materials show considerable range of values both for J as well as E.

Taking into account other factors such as the availability of wire in suitable sizes, cost of material and the convenience of fabrication, it is decided that initially the commutator will be made out of copper wires. About 20 wires of 0.005 inch diameter will be mounted between the rotary and fixed structure in a circle of radius equal to the electrode radius. The length of these wires will be made small allowing a little slack so as to reduce the current element intersecting the magnetic field lines at an angle. Ideally these wires should be parallel to the magnetic field. If, however, the wires are randomly oriented the forces produced by the magnetic field will tend to cancel out. These precautions are necessary to minimize the homopolar and electromagnetic forces in the commutator which may otherwise result in false measurements of the drag forces.

Table 1

Relative Figure of Merit for Commutator Material

Material	Melting[a] Point T_m(°K)	Specific[b] heat S(cal/gm°C)	Density[c] d(gm/cc)	Resistivity[d] ρ(ohm cm) x 10^{-6}	Modulus of[b] Elasticity E(dynes/cm^2) x 10^{11}	Figure of[e] Merit J(amp/cm^2) x 10^2
Aluminum	932	0.225	2.7	2.8	5 – 8	57.1
Beryllium	1556	0.425	1.8	10.1	——	49.7
Cadmium	594	0.056	8.6	7.4	6.9	24.6
Chromium	2176	0.111	7.2	13.0	24.8	53.0
Cobalt	1768	0.107	8.7	9.7	——	59.7
Copper	1357	0.094	8.9	1.8	10 – 12	109.0
Gold	1336	0.032	19.3	2.4	7.8	79.5
Iridium	2727	0.032	22.4	6.1	5.2	82.5
Iron	1809	0.115	7.9	10.0	8 – 10	57.5
Managanese	1517	0.121	7.3	5.0	——	71.7
Molybdenum	2890	0.065	10.2	5.7	29.4	85.2
Nickel	1725	0.115	8.8	6.1	20 – 22	75.2
Osmium	3318	0.031	22.5	60.2	——	91.5
Palladium	1823	0.056	12.2	11.0	11.8	47.7
Platinum	2043	0.034	21.3	10.0	16.7	54.8
Rhenium	3453	0.035	20.5	18.6	——	54.0
Rhodium	2239	0.058	12.4	4.7	29.4	84.3
Silver	1234	0.056	10.5	1.6	7.7	90.0
Tantalum	3270	0.036	16.6	13.8	18.6	55.5
Titanium	1940	0.112	4.5	3.2	——	78.8
Tungsten	3650	0.032	19.3	5.5	35.5	95.8
Uranium	1406	0.029	18.7	29.0	——	22.2
Vanadium	2190	0.115	5.9	19.9	——	39.5
Zirconium	2128	0.068	6.4	42.4	——	21.3

[a] R. E. Honing, R.C.A. Review, 23, 574 (1962).

[b] Handbook of Physics and Chemistry, 38th Ed. (1956 – 57).

[c] A.I.P. Handbook, Second Ed. (1963) p. 2 – 19.

[d] A.I.P. Handbook, Second Ed. (1963) p. 9 – 38.

[e] $$J = \left[\frac{s \cdot d \, (T_m - T_o)}{\rho} \right]^{1/2}$$

2.1.2   Electrical Circuit for Pulsed Plasma Discharge

Figure 2 illustrates the electrical circuit for generating high current arc pulse using a condenser discharge.

Initially a 90 μ fd - 5 kV condenser bank will be charged by the high voltage power supply through a resistor R (limiting the maximum charging current to the power supply rating).   For a 200 ma power supply the charging time is given by:

$$t_{ch} = \frac{Q}{i} = \frac{S \times 10^3 \times 90 \times 10^{-6}}{0.2} = 2.25 \text{ sec.}$$

The charged condenser will then be connected to the arc circuit consisting of an L-R-C network.   For the purpose of analysis it is assumed that all the inductances and resistances are lumped in L_1 and R_1 respectively. The following relations govern the conditions of a critically damped discharge[4]:

a)   The discharge is critically damped when

$$R^2 = \frac{4L}{C} \quad , \tag{3}$$

b)   The current I through the circuit is given by

$$I = \frac{2V}{R} \frac{t}{T} e^{-t/T} \tag{4}$$

where the time constant $T = \frac{2L}{R}$, and

c)   The peak current, $I_{peak} = \frac{2V}{R} e^{-1}$ at $t = T$, and $I \simeq 0$ at $t \simeq 5T$.

The resistance R_1 for a peak current of 1000 amps from the 5kV charged condenser is;

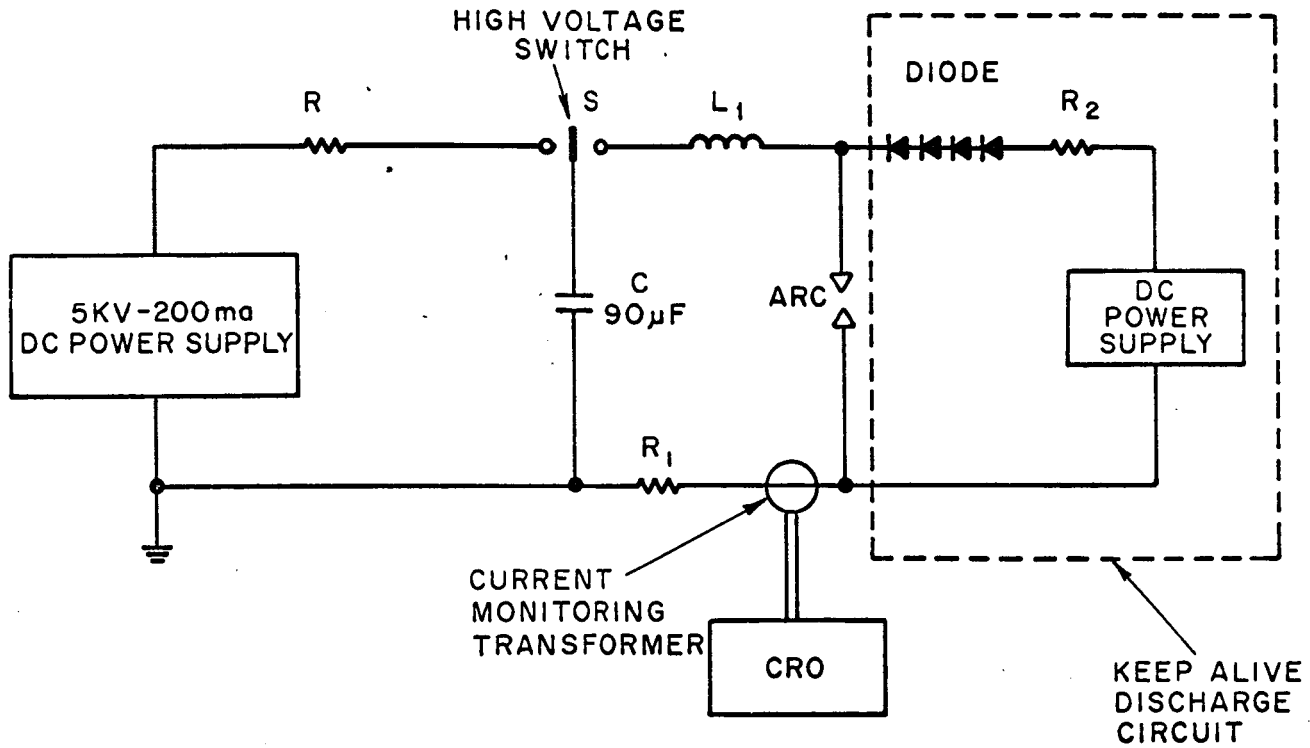$$R_1 = \frac{2V}{I_{peak}} e^{-1} = \frac{2 \times 5 \times 10^3}{10^3 \times 2.7} = 3.7 \text{ ohms.}$$

FIGURE 2.

CIRCUIT DIAGRAM FOR PRODUCING PULSED PLASMA DISCHARGE.

The inductance L_1 for a critically damped condition is

$$L_1 = \frac{R_1^2 C}{4} = \frac{(3.7)^2 \times 90 \times 10^{-6}}{4} = 3.08 \times 10^{-4} \text{ henries,}$$

and the time constant

$$T = \frac{2L_1}{R_1} = \frac{2 \times 308 \times 10^{-6}}{3.7} \simeq 1.7 \times 10^{-4} \text{ sec .}$$

The pulse magnitude, duration and the shape can be controlled by adjusting the condenser charging voltage V, the inductance L_1 and the resistance R_1 in the circuit. The arc current and its duration will be measured with a Pearson current monitor transformer and a Tektronix CRO.

A "keep alive" discharge circuit is also included in this system. The purpose of this unit is to maintain a continuous glow discharge of a few milliampere between the main arc electrodes. It is planned that in this way every time when the condenser is triggered for a pulse discharge it is sure to fire. A string of diodes is included in this circuit to prevent the high voltage from appearing at the "keep alive" power supply. The resistance R_2 limits the glow discharge current to a suitable level.

2.1.3 The Drag Force Measurement in a Ballistic Mode

From the basic mechanics, if M is the moment of interia of the force transducer and P is the momentum due to an impulse force F of duration Δt then the kinetic energy imparted to the system is;

$$K \cdot E \cdot = \frac{1}{2} \frac{P^2}{M} = \frac{1}{2} \frac{(F \Delta t)^2}{M} . \tag{5}$$

In addition, if k is the spring constant and θ_o the angular displacement produced by the force, then the potential energy stored in the system is;

$$P \cdot E \cdot = \frac{1}{2} k \theta_o^2 . \tag{6}$$

Equating the kinetic and potential energies and solving for θ_o, one gets

$$\theta_o = \frac{P}{\sqrt{kM}} \simeq \frac{F \Delta t}{\sqrt{kM}} . \tag{7}$$

The period of oscillation for an undamped oscillation is

$$T_o = 2\pi \sqrt{M/k} = \frac{2\pi}{\omega} \tag{8}$$

and for a damped oscillation is;

$$T_1 = \frac{2\pi}{\sqrt{\omega^2 - c^2}} = \frac{T_0 \omega}{\sqrt{\omega^2 - c^2}} \tag{9}$$

where c denotes the damping term. Further, a steady deflection θ_{st} produced by a steady force F_{st} is given by;

$$\theta_{st} = F_{st}/k . \tag{10}$$

From Equations (7), (8), and (10) it follows that;

$$\theta_o = \frac{2\pi}{T_0} \cdot \frac{\theta_{st}}{F_{st}} \cdot P = \frac{2\pi}{T_0} \cdot \frac{\theta_{st}}{F_{st}} \cdot F \Delta t . \tag{11}$$

Knowing θ_o, θ_{st}, F_{st} and T_0 from experiment will permit an evaluation of P or the impulse force F.

In the earlier measurement[1] using a similar transducer structure, a force F_{st} of 2 gm cm/sec^2 produced a signal of 0.07 volts corresponding to a deflection θ_{st}. The period of oscillation T_0 of this structure was about 0.5 sec. Substituting these values in Equation (11), a voltage signal V_o corresponding to the deflection θ_o is given by;

$$V_o \simeq 0.44 \, F \, \Delta t. \tag{12}$$

The force F produced by ions at the cathode from a 1000 amp arc can be estimated using the expression

$$F = \sigma \, (mv) \frac{1}{e} \, f \tag{13}$$

where σ is the tangential accommodation coefficient (assumed to have a value of unity), (m v) is the momentum carried by each ion and f is the fraction of current carried by the ions. The value of f was estimated to be about 10% from the earlier measurements[1]. For an argon ion moving with a tangential velocity $v \simeq 8.71 \times 10^5$ cm/sec, the force f is expected to be 3.6×10^4 gm cm/sec^2 for a 1000 amp arc. If the pulse duration is about 2×10^{-4} sec, the expected voltage signal V_o is about 3.16 volts. Since a signal of this magnitude can be conveniently measured, no difficulties are anticipated in the drag force measurements using this technique.

2.2 Measurement of Particle Velocity in the Plasma by Doppler Shift Techniques

The usefulness of measuring the particle velocity in the plasma accelerator has been discussed earlier in a report[5]. Several methods of measuring velocity are considered in that report and it is concluded that the most sensitive and direct method for this purpose would be the Doppler shift

technique. The theory of Doppler effect states that the shift $\Delta\lambda$ in a wavelength λ from a source moving with a velocity v is given by

$$\Delta\lambda = \lambda\, v/c \tag{14}$$

where c is the velocity of light ($= 3 \times 10^{10}$ cm/sec). Thus if λ and $\Delta\lambda$ are known from the experiment, the velocity v can be computed.

Typically in a plasma the velocity v is of the order of 10^{6} cm/sec, so that the expected shift $\Delta\lambda$ in the visible range ($\lambda \simeq 5000\overset{o}{A}$) is of the order of $0.2\overset{o}{A}$. An experiment employing a Fabry-Perot interferometer is designed to study the shift $\Delta\lambda$ in the wavelength λ.

Figure 3 shows the electrode structure and the optical arrangement to bring the plasma radiation out from the arc vacuum chamber. The instrumentation for the Doppler shift experiment is designed to suit the coaxial plasma accelerator that was used for the electrode drag force measurement. In this way the results of velocity measurement can be directly applied to interpret the results of drag measurement. The light from the plasma is collected by a hollow stainless tube at an angle of 45° to observe a significant component of the velocity vector along the line of sight. The light collected from the moving plasma goes into an optical system consisting of narrow band filters and interferometers etc.

Suppose that initially the optical probe is receiving light from the plasma moving towards the probe. If now the direction of motion of the plasma is reversed by changing the direction of magnetic field vector, the probe will collect light from the plasma moving away from it. The resultant change in the wavelength $\Delta\lambda$ due to the change in the direction of the flow of plasma will correspond to twice the Doppler shift in the wavelength λ. Although a single light probe is sufficient to study the particle velocity in the plasma, several
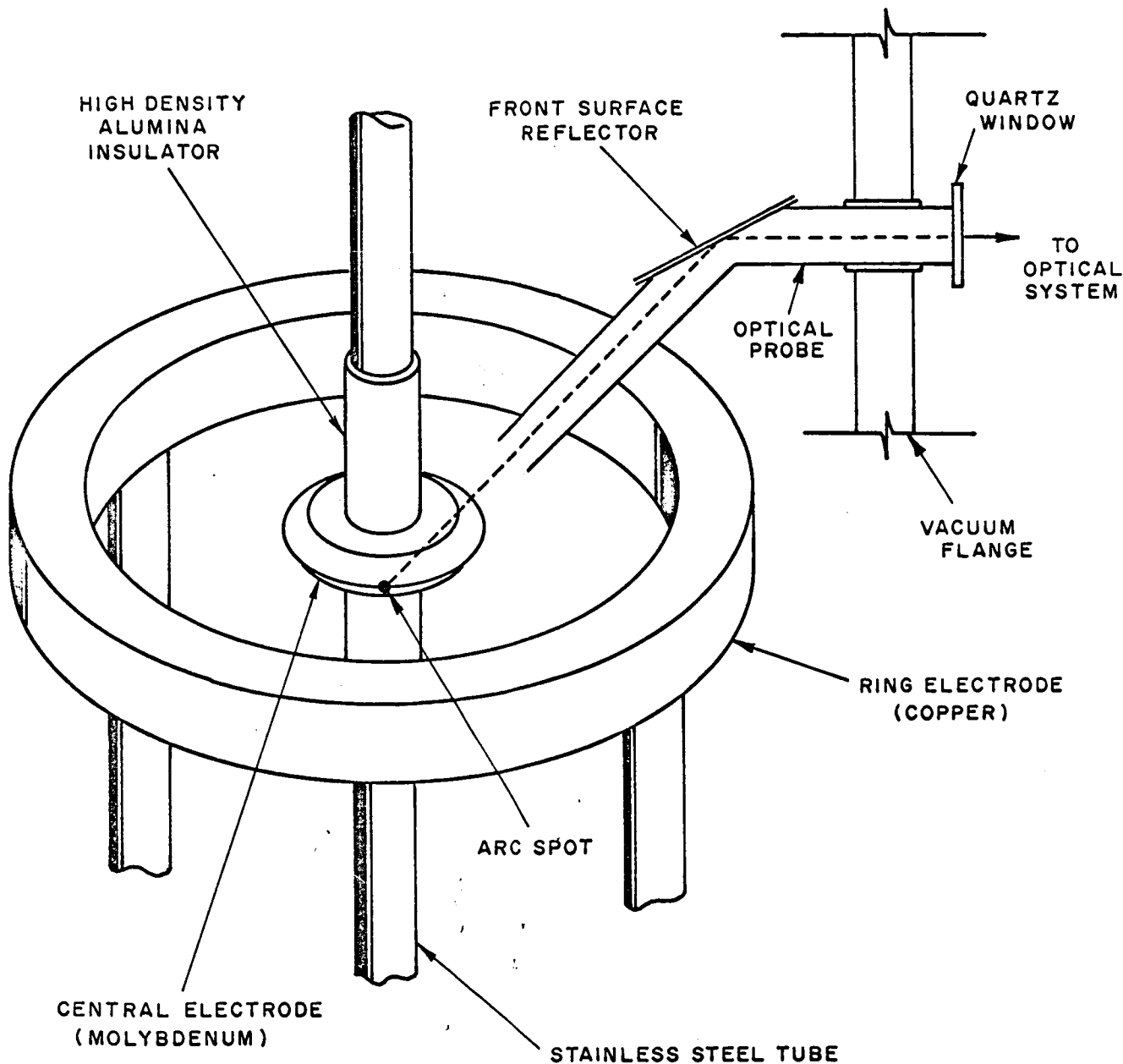
FIGURE 3.

ELECTRODE GEOMETRY AND OPTICAL PROBE
ARRANGEMENT FOR THE PATICLE VELOCITY
MEASUREMENT BY DOPPLER EFFECT.

ACE SCIENCES INCORPORATED

light probes are provided to check the internal consistency of the measurement. The apparatus is built with sufficient flexibility so as to be able to study any segment of the plasma. The details of the system required to determine $\Delta\lambda$ are discussed in the following sections.

2.2.1 Electro-Optical System for Doppler Shift Measurement

As noted earlier, to determine the particle velocity, it is necessary to measure the shift $\Delta\lambda$ in the wavelength λ of the moving particle. For this purpose a wavelength λ should be selected which is strongly radiated and also fairly well isolated from other lines. A list of argon lines along with their relative intensities is given in Table 2. This table suggests several possibilities. Tentatively it is decided to study the shifts covering a wide range of spectrum. Once again, although the complete information can be obtained only with one line, the second line is included to check the internal consistency of these measurements.

The system consisting of a Fabry-Perot interferometer and other optical elements is shown in Figure 4. The lens L_1 renders the light from the arc source S into a parallel beam of light which then goes through a narrow band filter F. The filter F is a 100 $\overset{o}{A}$ wide interference filter which can be tuned to a required wavelength by changing the angle of incidence. According to the manufacturer, a typical change of 20° in the angle of incidence shifts the transmission peak by about 100 $\overset{o}{A}$.

The filtered light goes into the Fabry-Perot etalon producing the interference ring pattern of dark and bright fringes. A scanning interferometer model F-103 commercially available from Electro-Optics Associates has been purchased by Space Sciences Incorporated for this purpose. The operating range of this instrument is from 4000 $\overset{o}{A}$ to 9500 $\overset{o}{A}$ and it features a magnetic reflector drive producing a $\lambda/2$ scan per volt. The cavity length in this unit can be varied from 0 to 100 mm continuously.

Table 2

Spectral Lines in Argon Discharge

Atomic Lines (Å)	Relative Intensity*
8424	1.8×10^6
8408	1.9×10^6
8264	1.5×10^6
8115	2×10^6
8103	1.6×10^6
7948	1×10^6
7723	1.2×10^6
7635	1.5×10^6
7383	9×10^5
7067	5×10^5
6965	7×10^5
6416	7×10^3
5606	2×10^3
5945	2×10^3
4702	1.9×10^3
4510	4×10^3
4300	1×10^4
4200	3×10^4
4158	3×10^4
3948	4×10^4

---

* American Institute of Physics Handbook, Second Ed. (McGraw Hill, New York, 1963).
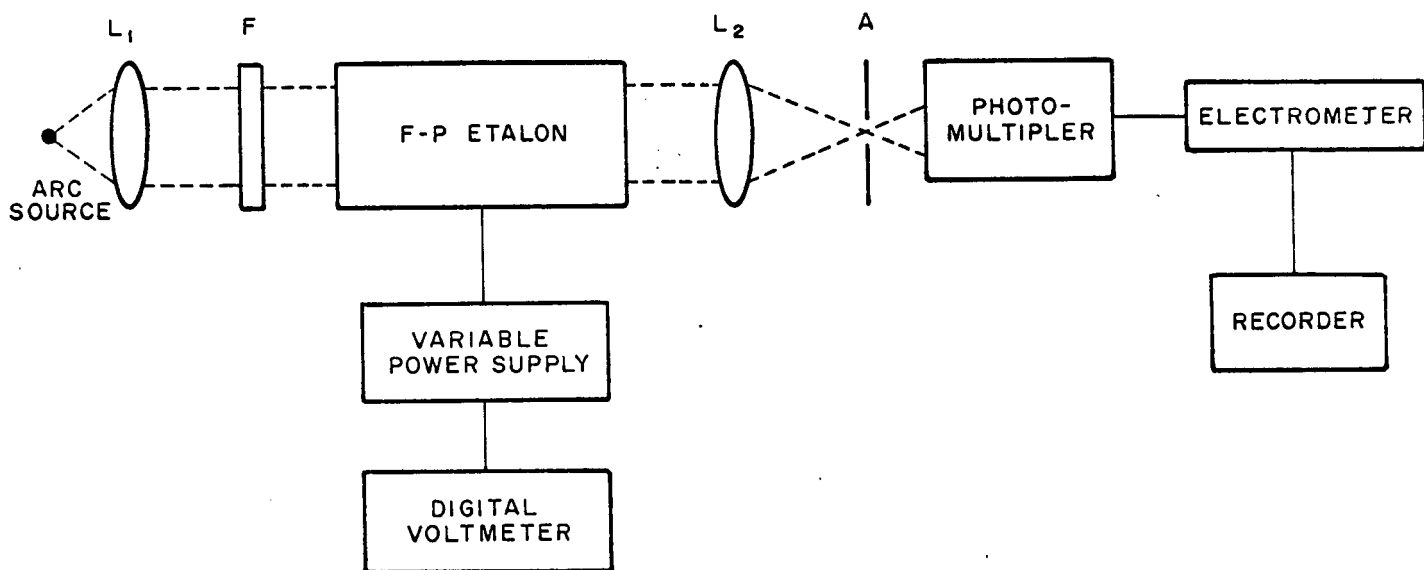
FIGURE 4.

SCHEMATIC OF THE APPARATUS TO
MEASURE DOPPLER SHIFT.

The fringe pattern is focused at a small aperture A by the lens L_2. A photomultiplier tube type 7102 RCA with S_1 characteristic detects the light signal passing through A. For improved signal-to-noise ratio the photomultiplier is cooled to dry ice temperature.

Since the rotating plasma produces a pulsed light signal, it is necessary to incorporate an average or pulse stretching pulse reading circuit. A positive peak detecting circuit conssiting of an operation amplifier and a solid state diode is shown in Figure 5. The output from this unit goes into an amplifier which drives a strip chart recorder.

A regulated power supply drives the magnetic reflector of the Fabry-Perot etalon. The voltage required to shift the fringes is read accurately on a digital voltmeter.

The condition for interfering fringes to produce a maxima at the aperture is

$$2 \, d\mu \cos \theta = n \lambda \tag{15}$$

where;

       d = cavity length of distance between the etalon plates,

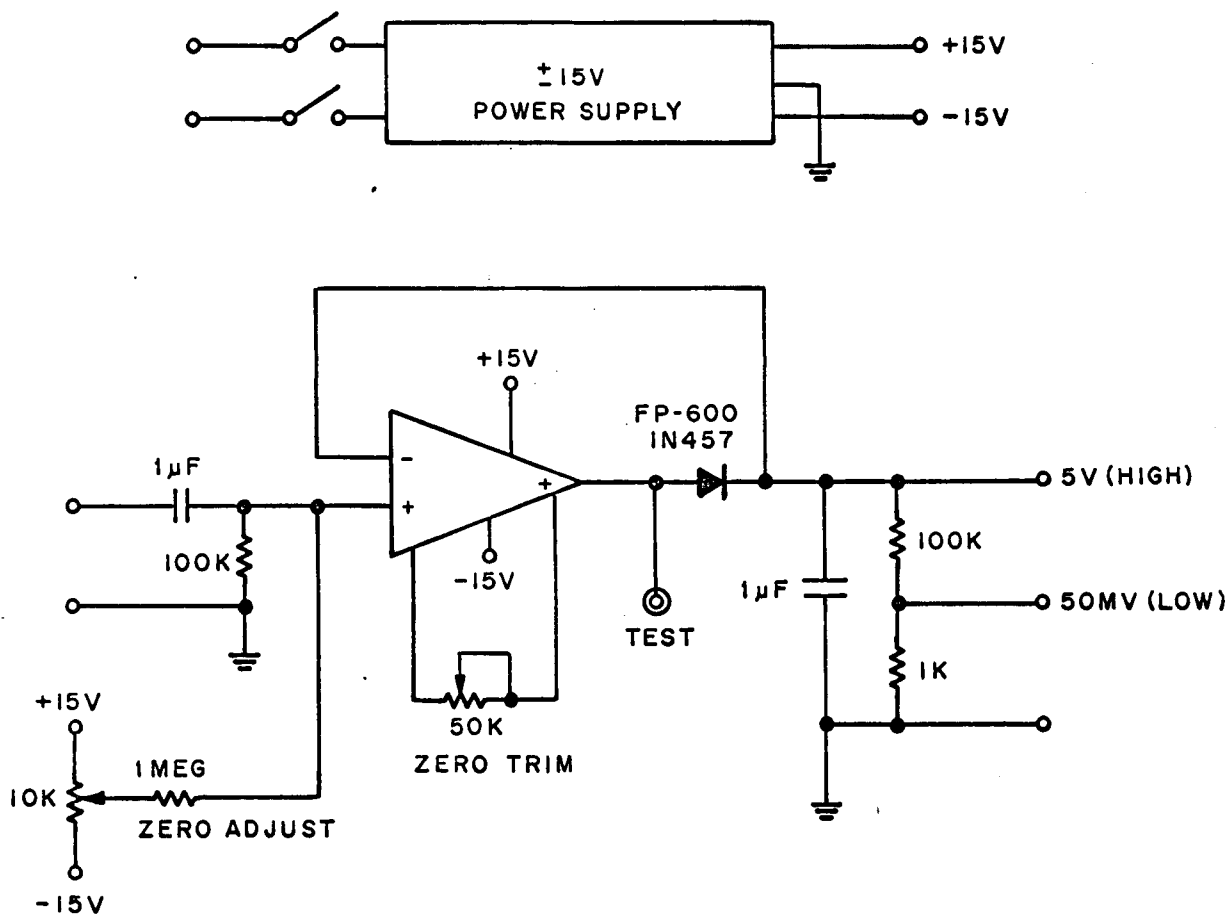 μ = refractive index of the medium between plates,

       θ = angle of incidence,

       n = order of interference, and

       λ = wavelength.

For a particular case if $\mu = 1$ (air) and $\cos \theta = 1$ (normal incidence) then Equation (15) reduces to

$$d = \frac{n}{2} \lambda \tag{16}$$

OPERATIONAL AMPLIFIER: ANALOG NO. 110A.

FIGURE 5.

POSITIVE PEAK DETECTOR.

Also for a fixed n, small changes in d and λ are given by;

$$\Delta d = \frac{\Delta\lambda}{\lambda} \ d \ . \tag{17}$$

Initially for a given λ, the interferometer is tuned to produce a bright fringe at the detector, thus defining exactly the value of n and d. A shift $\Delta\lambda$ in λ then causes an unbalanced condition in the detector. The system is balanced again by adjusting d to produce the same peak signal in the detector. The change Δd required to bring the signal to its original level is measured in terms of voltage signal.

Consider, for example, that the instrument is tuned for a maxima with $d = 1$ cm, and $\lambda = 8000 \overset{o}{A}$. The corresponding value of n, the order of interference is;

$$n = \frac{2d}{\lambda} = \frac{2 \times 1}{8 \times 10^{-5}} = 2.5 \times 10^4 \ .$$

If the particle velocity $v = 10^6$ cm/sec, the shift $\Delta\lambda$ due to Doppler effect is;

$$\Delta\lambda = \frac{\lambda v}{c} = \frac{8 \times 10^{-5} \times 10^6}{3 \times 10^{10}} \simeq 2.7 \times 10^{-9} \text{ cm,}$$

and Δd required to bring the same fringe into position is

$$\Delta d = \frac{\Delta\lambda}{\lambda} \ d = \frac{2.7 \times 10^{-9} \times 1}{8 \times 10^{-5}} = 3.3 \times 10^{-5} \text{ cm.}$$

According to the manufacture of the interferometer etalon, a 1 volt signal on the magnetic reflector drive scans a distance of $\lambda/2 = 4 \times 10^{-5}$ cm. The expected voltage signal for $\Delta d = 3.3 \times 10^{-5}$ cm will therefore be about 0.83 volts.

In order to avoid the possibilities of confusing the interference fringe order it is necessary to adjust d so that Δd is much less than $\lambda/2$.

It will be useful to calibrate the instrument so that the voltage signal can be directly related to the wavelength shift $\Delta\lambda$. This can be done by plotting the voltage required to bring the successive interference fringes into the detector. The $V - \lambda$ curve will then yield an absolute calibration of the entire system for a given wavelength.

Several techniques have been conceived to determine the shift in the peak signal. In addition to measuring the dc signal with an electrometer, it is also possible to excite the magnetic reflector drive with an ac signal and study the corresponding shift with a CRO. A shift in $\Delta\lambda$ in this case will produce a shift in the CRO trace which can be restored by adjusting the dc bias on the reflector drive. A phase sensitive tuned amplifier will also be employed to study the fringe pattern in case the background noise masks the signal on the CRO. Depending upon the signal to noise ratio, various techniques will be employed for this measurement.

3. ENERGY DEPENDENCE OF THE ACCOMMODATION COEFFICIENT

Based upon an examination of the physical processes involved in the transfer of energy and momentum between a plasma particle and the plasma boundary, it is concluded that the accommodation coefficients (energy and momentum) are functions of energy for sufficiently high velocities. The experimental measurements of the tangential electrode drag has shown the presence of a threshold transverse magnetic field and arc current at which the tangential drag suddenly increases. An examination of possible reasons for the observed drag threshold has led to the realization that at sufficiently large particle velocities a sudden change of accommodation coefficients can be predicted.

The increase in accommodation coefficient can be related to the case where the energy transferred to an electrode (or target) atom becomes large enough to overcome the surface bonding energy of the target atom. The energy and momentum transferred to a relatively mobile atom is expected to be much different from the energy transferred to a locally bound atom.

The energy threshold for the target atom to become surface mobile is related to the melting temperature of the target material. This threshold energy is less than the latent heat of vaporization since it involves only two dimensional motion rather than 3 dimensional motion. This threshold surface energy is expected to be about 0.1 to 0.4 electron volts for various target materials. Assuming that there is an energy accommodation coefficnt of about 0.5 (depending upon the incident particle mass and the target mass) the incident particle energy corresponding to this threshold energy is about 0.2 to 0.8 electron volts. For gas of molecular weight of about 40, the corresponding gas velocity is 1×10^5 to 2×10^5 cm/sec for the assumed range. Assuming the velocity of $C_o = 3.316 \times 10^4$ cm/sec as corresponding to Mach 1 for air at 0°C and at 1 atmosphere, the corresponding range of Mach No. is about 3 to

6 Mach. Thus it is expected that the threshold accommodation coefficient will occur in the representative range for high speed plasmas in accelerators and MHD energy converters and high speed re-entry and orbital vehicles.

A more detailed analysis of the threshold accommodation coefficients is in progress as related to the observed threshold in electrode drag. The surface atom energy corresponding to the drag threshold is being formulated in terms of the Debye temperature of the surface material θ_D, the atom weight, and the atomic radius. In the process of analysis, an explanation has been derived for the Lindemann equation used to describe the melting point T_m. This is because the same physical processes are active in melting and in the threshold accommodation coefficient.

In conjunction with a study of the accommodation coefficient, an analysis was made of the reported angular scattering of lower temperatures gases from various surfaces. A model was developed to predict the maximum scattering angle as a function of the incident beam temperature and the surface temperature, as well as the mass ratio. This model predicts the deviation of the scattering towards the normal and the deviation of the maximum from the specular scattering angle. For this model, the deviation of the calculated angles from the reported angles is about 1 to 2 degrees and is much smaller than the deviation reported for other theoretical models. This data is for low energy atoms (about 0.1 eV or less) and does not approach the accommodation coefficient threshold range. Further study of the problem of accommodation coefficient as related to the observed drag threshold is in progress.

REFERENCES

1) Rohatgi, V. K. and Aisenberg, S., "Ion Drag and Current Partitioning at the Cathode of a Plasma Accelerator," AIAA Paper No. 67-657 (1967).

2) Rohatgi, V. K. and Aisenberg, S., "Composite Metallic and Dielectric Insulator for High Current Arc Electrodes," Rev. Sci. Instr., 37, 1603 (1966).

3) Aisenberg, S., Hu, P., Rohatgi, V.K. and Ziering, S., " A Study of Electrode Effects in Crossed Field Accelerators," First Summary Report, Document No. SSI-152-SR (1965).

4) Starling, S. G., Electricity and Magnetizm (Longmans, Green and Co., New York, 1947) p. 337.

5) Aisenberg, S. Hu, P., Rohatgi, V. K. and Ziering, S., "Plasma-Boundary Interactions - II," to be published as a NASA Contractors Report.